Variable Stiffness Soft Pneumatic Sensing Chambers for Tactile Sensing and Haptic Devices

Supplementary material

S. Duretto, G. Colucci, L. Tagliavini, A. Botta, G. Quaglia

Appendix A: Elastic Force and Hysteresis

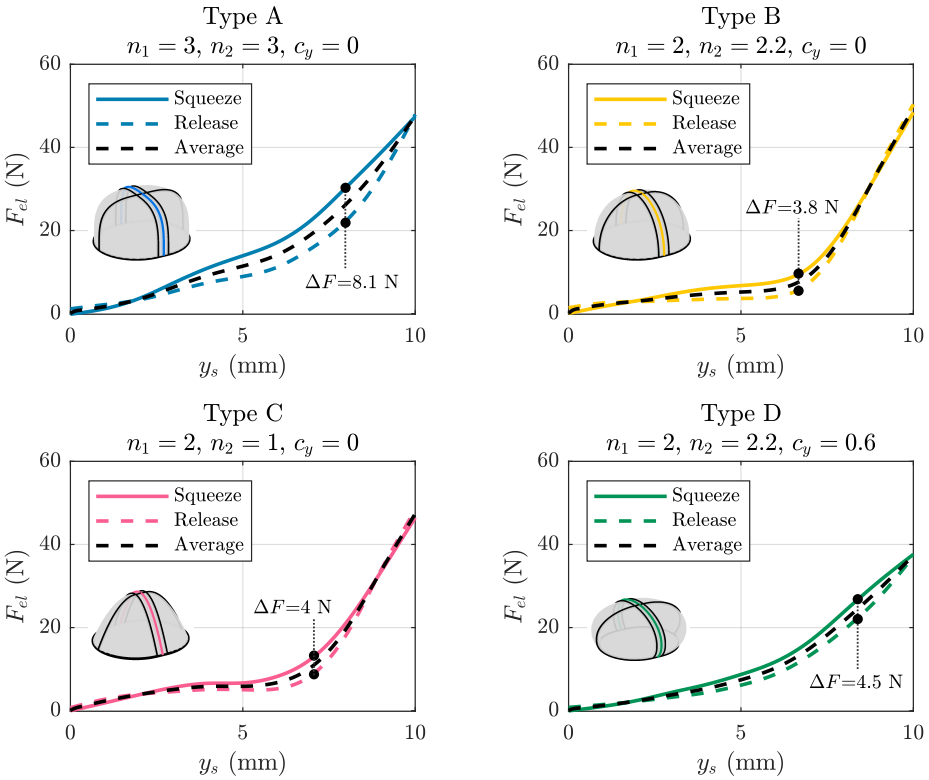

Figure 1: Elastic force over a squeezing cycle and maximum hysteresis for SPSCs made of Recreus TPU 60A, with $w = 11$ mm, $h = 13$ mm, $l = 3$ mm, $t_0 = 1$ mm, measured with the chamber open to the atmosphere.

Table 1: Hysteresis data for SPSCs made of Recreus TPU 60A

Type	ΔF_{max} (N)	$\mathcal{L}_{hys}$ (mJ)	$\mathcal{L}_{hys}/\mathcal{L}_{mean}$
A	8.1	36.2	0.24
B	3.8	13.7	0.12
C	4.0	11.5	0.10
D	4.5	20.3	0.18

ΔF_{max} = maximum hysteresis
$\mathcal{L}_{hys}$ = energy lost during a squeezing cycle
$\mathcal{L}_{mean}$ = average energy to squeeze the SPSC

Appendix B: Static Test Results

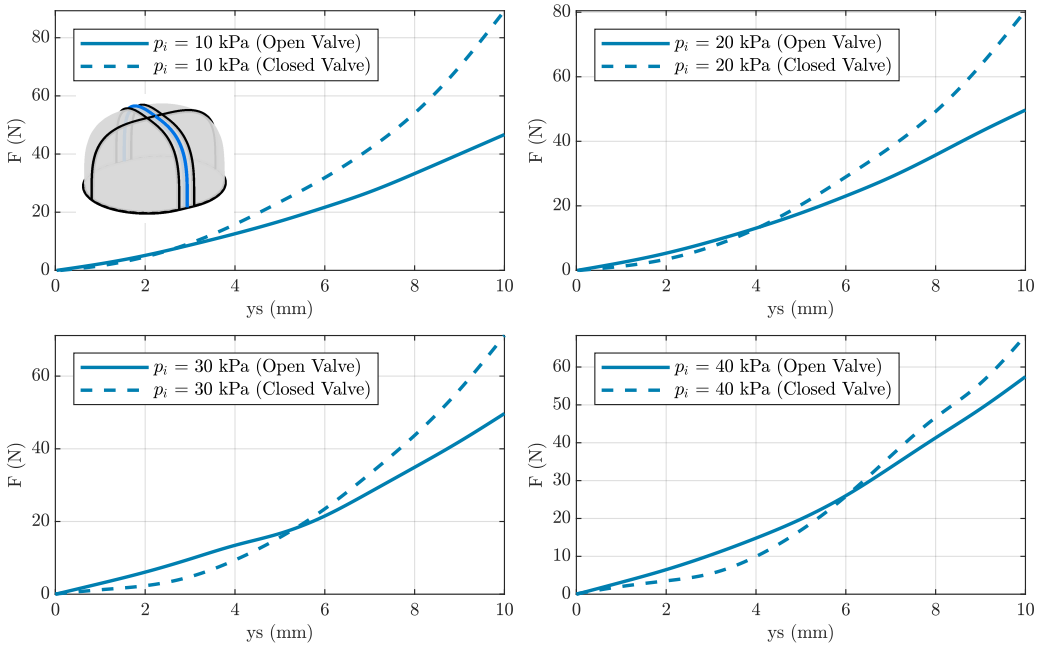

Figure 2: Experimental contact force measured for different inflation pressures p_i, in the low and high stiffness configurations. Type A SPSC made of Recreus TPU 60A.

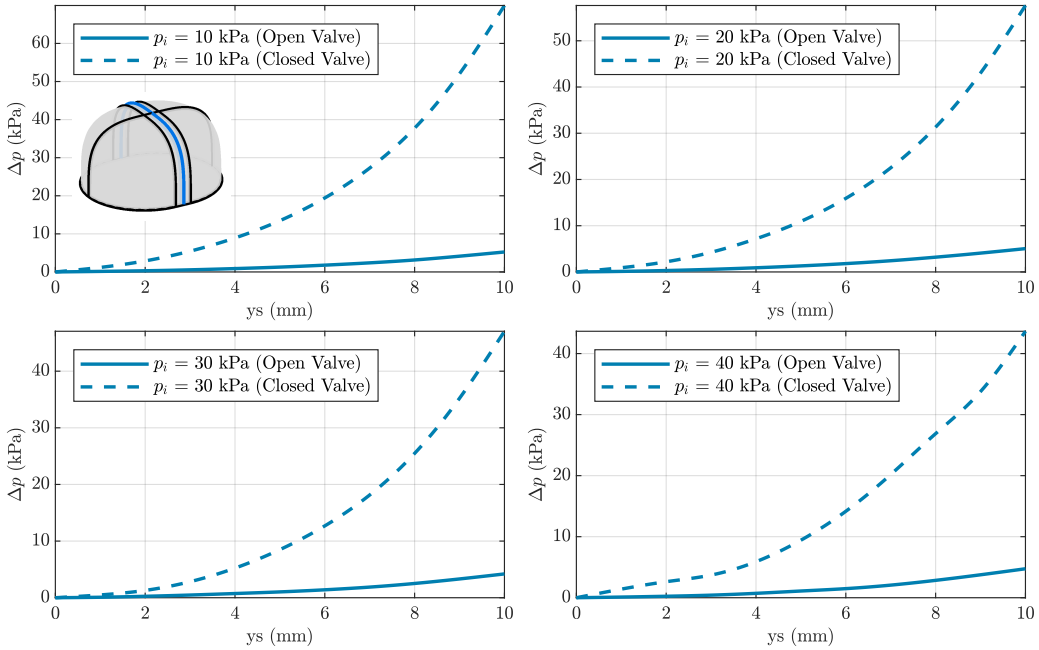

Figure 3: Experimental pressure change in the chamber measured for different inflation pressures p_i, in the low and high stiffness configurations. Type A SPSC made of Recreus TPU 60A.

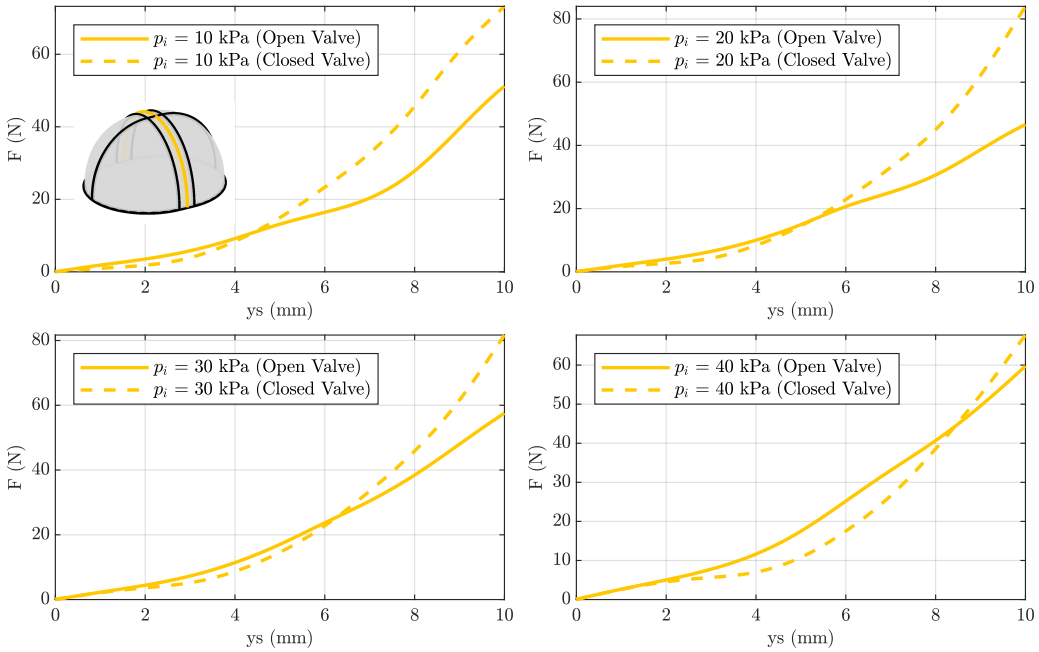

Figure 4: Experimental contact force measured for different inflation pressures p_i, in the low and high stiffness configurations. Type B SPSC made of Recreus TPU 60A.

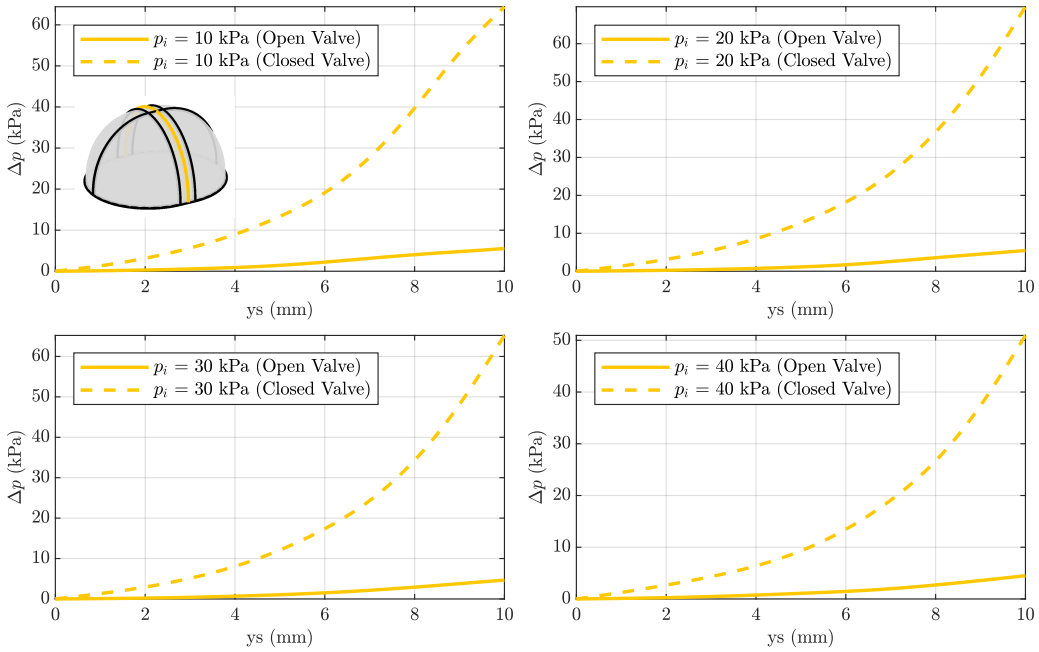

Figure 5: Experimental pressure change in the chamber measured for different inflation pressures p_i, in the low and high stiffness configurations. Type B SPSC made of Recreus TPU 60A.

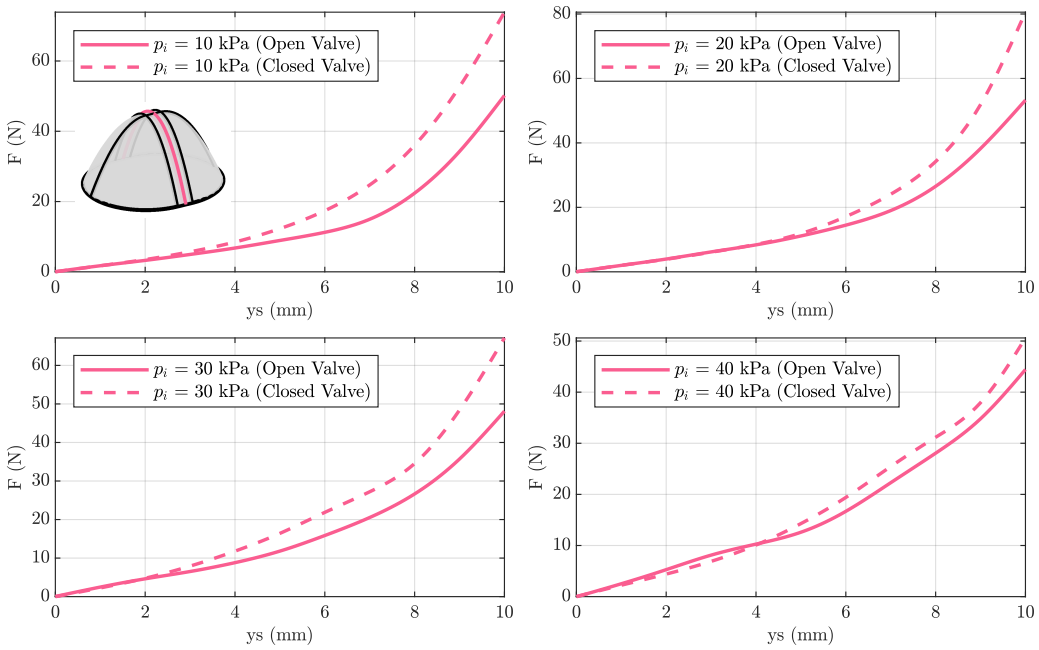

Figure 6: Experimental contact force measured for different inflation pressures p_i, in the low and high stiffness configurations. Type C SPSC made of Recreus TPU 60A.

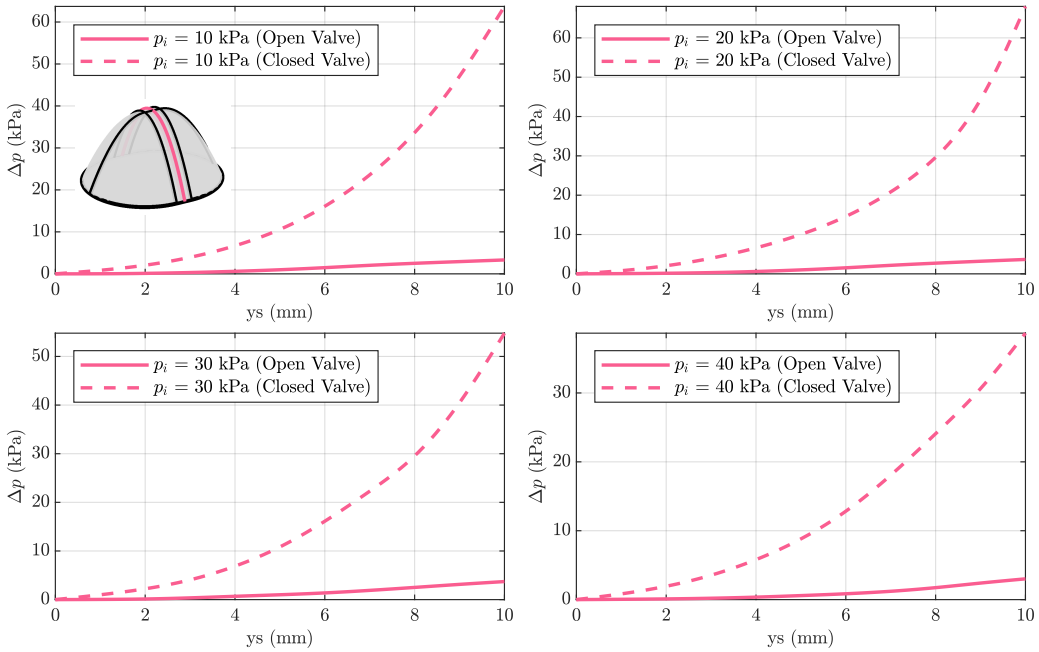

Figure 7: Experimental pressure change in the chamber measured for different inflation pressures p_i, in the low and high stiffness configurations. Type C SPSC made of Recreus TPU 60A.

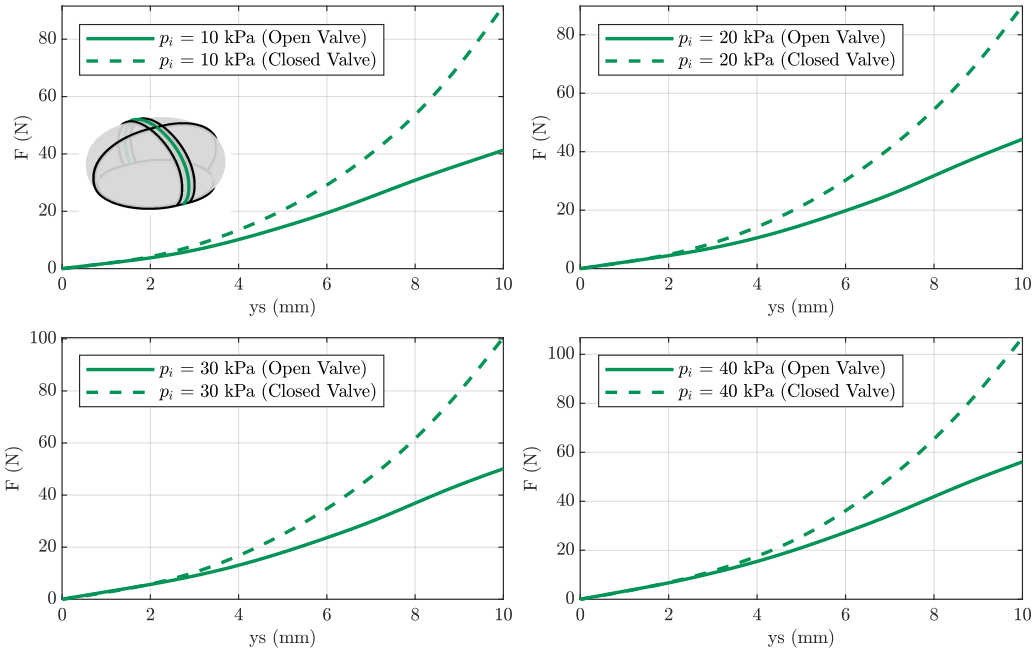

Figure 8: Experimental contact force measured for different inflation pressures p_i, in the low and high stiffness configurations. Type D SPSC made of Recreus TPU 60A.

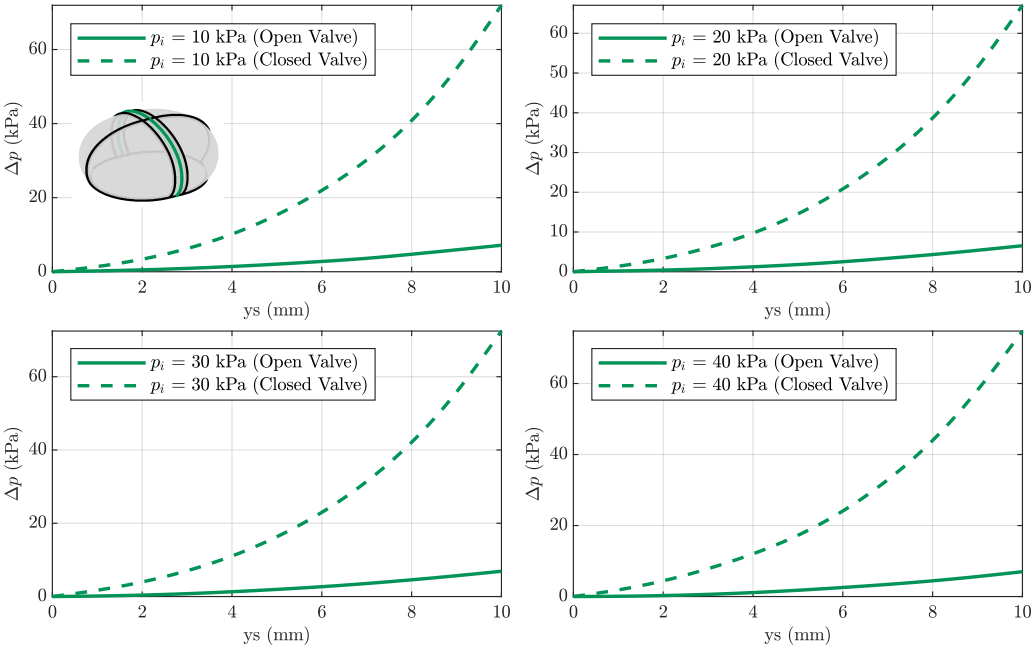

Figure 9: Experimental pressure change in the chamber measured for different inflation pressures p_i, in the low and high stiffness configurations. Type D SPSC made of Recreus TPU 60A.

Appendix C: Performance Estimate from Test Data

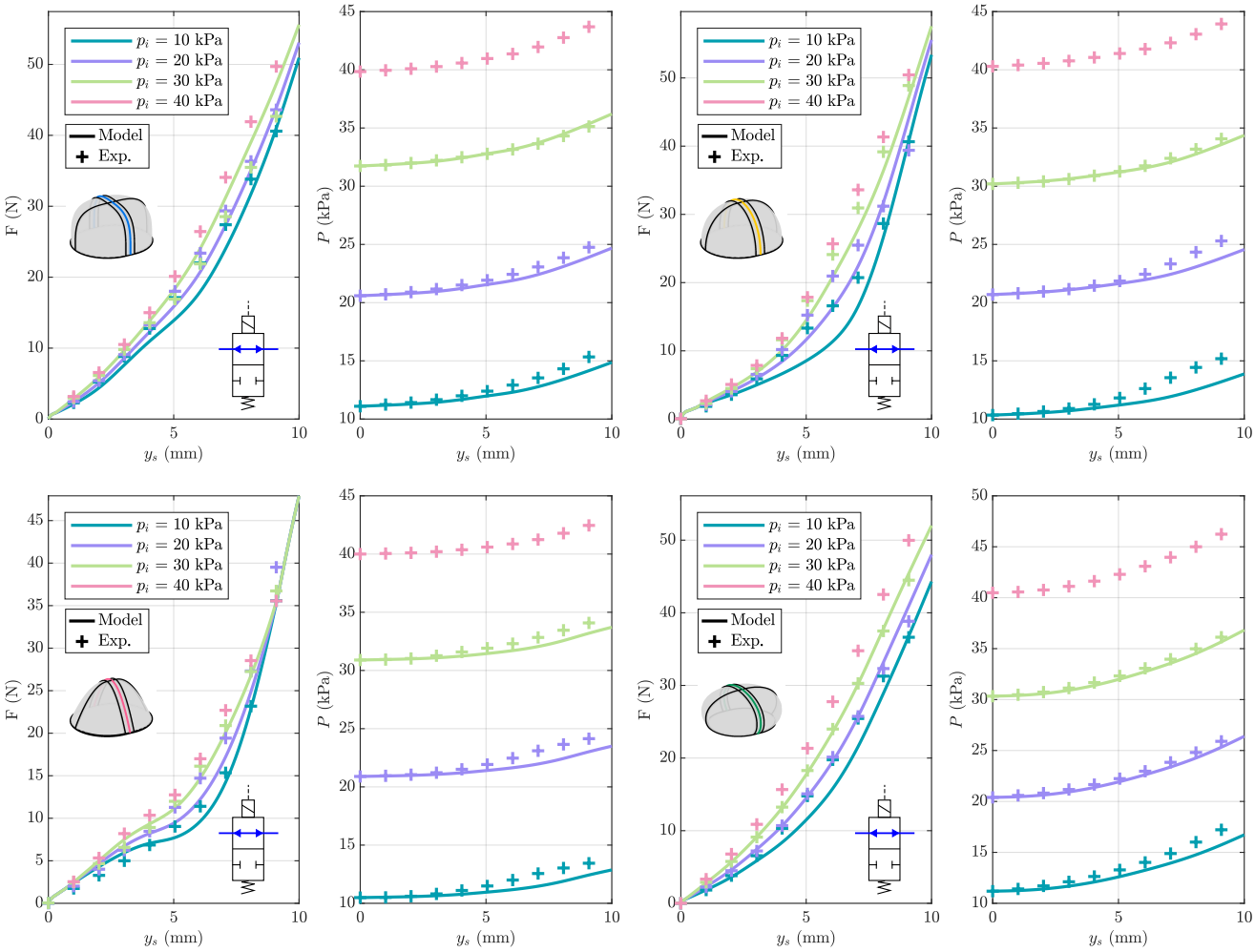

Figure 10: Contact force and gauge pressure estimated starting from the static test at $p_i = 40$ kPa in the low stiffness configuration, for SPSC Types {A, B, C, D} made of Recreus TPU 60A.

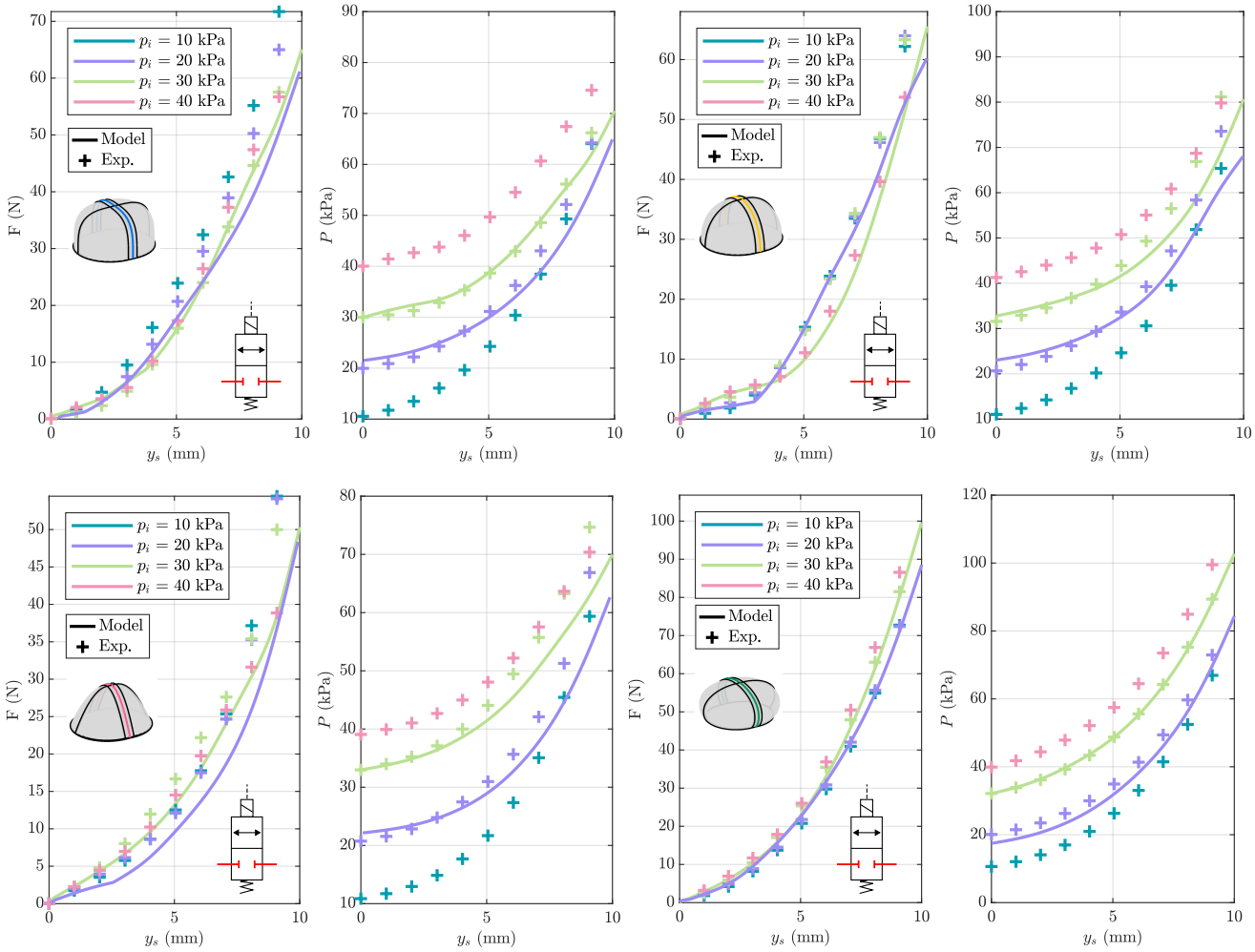

Figure 11: Contact force and gauge pressure estimated starting from static tests, in the high stiffness configuration. To get better estimates, the quantities for $p_i = 20$ kPa were estimated from the test at $p_i = 10$ kPa, while the quantities for $p_i = 30$ kPa were estimated from the test at $p_i = 40$ kPa. SPSC Types {A, B, C, D} made of Recreus TPU 60A.

Appendix D: Manufacturing of the SPSCs

The fabrication process for the SPSCs used in this work is detailed below.

Compression molding

SPSCs made from platinum cure RTV silicone AS40 (supplied by Easy Composites) were manufactured through a multi-step process using a 3D-printed mold consisting of two parts, as shown in Fig. 12(a). Silicone parts A and B were mixed according to the manufacturer's instructions. Then, the mixture was degassed in a vacuum chamber for 15 minutes and subsequently poured into the lower part of the mold, shown in red. The upper part of the mold, shown in blue, presents a punch that forces the liquid silicone to fill the meatus between the two parts of the mold. Four prismatic couplings ensure correct alignment between the two parts of the mold, and the lower part also features a channel for collecting excess silicone. Moreover, a cotton gauze was placed inside the mold to strengthen the membrane. The gauze was placed in the mold halfway through the silicone casting process, then covered with the remaining quantity of silicone. The curing process was carried out at room temperature (23 °C). Finally, the SPSC was closed by means of rigid attachment with a rigid lower base, as depicted in Fig. 12(b). Any minor air leaks were prevented by means of two-component glue.

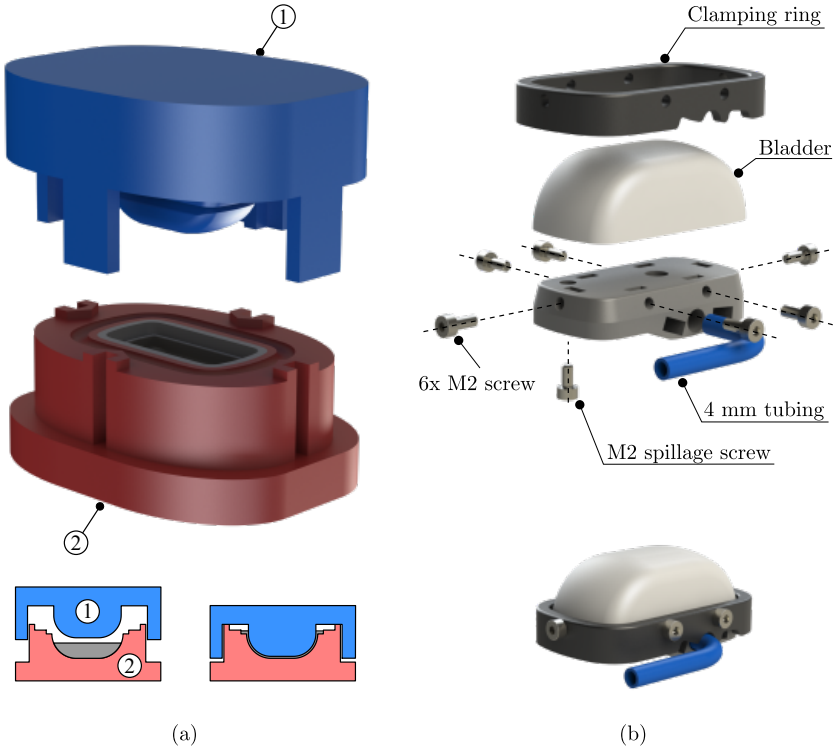

Figure 12: (a) Exploded view of the molds for the production of SPSC in silicone. (b) Exploded view of the SPSC assembly.

FDM

SPSCs made from Filaflex TPU 60A (supplied by Recreus Industries S.L.) were manufactured through Fused Deposition Modeling (FDM) technology using a Bambu Lab X1-Carbon equipped with a 0.4 mm nozzle. Printing files were generated through the Bambu Studio slicer using custom-defined printing settings (Table 2). Additional post-processing steps were performed to ensure air tightness. Specifically:

1. localized melting of the SPSC's outer surface by a soldering iron, with temperature set at 200 °C;
2. injection of a liquid latex sealant (PMP Orange Latex) inside the SPSC's chamber. The excess liquid was then drained out.

The process was repeated until the desired degree of air tightness was obtained.

Table 2: 3D Printing Process Parameters

Parameter	**Value**
Flow ratio	1.6
Print temperature	245 °C (all layers)
Build plate temperature	35 °C (Textured PEI Plate)
Max volumetric speed	1.6
Fan speed	100%
Retraction length	0.4 mm
Retraction speed	35 mm/s
Travel distance threshold	2.5 mm
Order of walls	outer/inner
Infill density	100%
Infill pattern	Concentric
Supports	Disabled

SLA

SPSCs made from Elastic 50A and Silicone 40A (both supplied by Formlabs) were fabricated through Stereolithography (SLA) technology using a Formlabs 3B+. Printing files were generated using the PreForm slicing software. Both Elastic 50A and Silicone 40A variants were printed using default settings, with post-processing (washing and curing) following standard Formlabs protocols.

Appendix E: Reliability Testing

The test bench used for reliability assessment is depicted in Fig. 13, and the resulting damage incurred to SPSCs is reported in Fig. 14.

Fatigue tests resulted in damage primarily between the 3D-printing layers for both TPU 60A and Elastic 50A specimens. However, TPU 60A SPSCs experienced minor damage, while Elastic 50A SPSCs experienced total membrane failure. A similar outcome was observed during the puncture tests.

Repairability of damaged specimens was also assessed based on the material type and the extent of the damage:

- TPU 60A: repair was possible via local melting and the application of additional TPU using a soldering tip;
- Silicone (Compression Molding/SLA): damaged areas were successfully sealed with a silicone sealant;
- SLA-Printed Materials: for materials printed via SLA, minor damage can often be repaired by locally applying the original resin and UV curing. However, extensive damage observed for Elastic 50A proved irreparable.

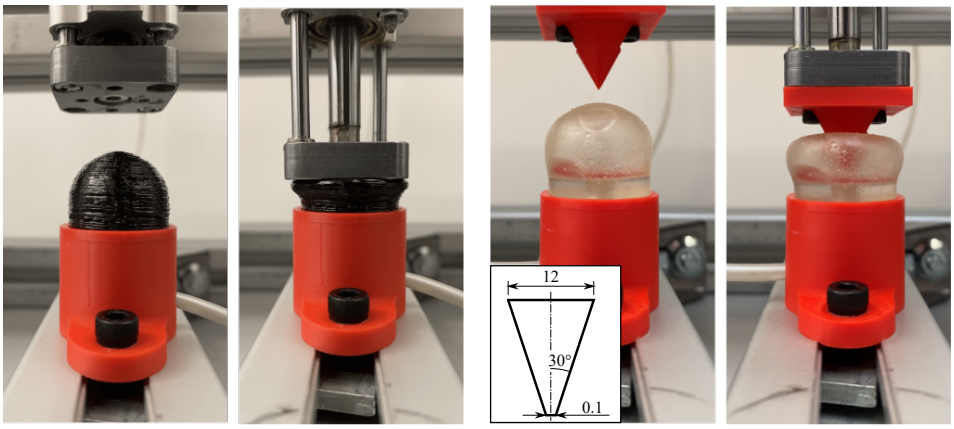

Figure 13: Reliability testing: (a) fatigue test (Type B SPSC made of Recreus TPU 60A), (b) puncture test (Type B SPSC made of Formlabs Elastic 50A). The conical probe is made of tough PLA material, with tip diameter of 0.1 mm, half angle of 30 deg and a base diameter of 12 mm.

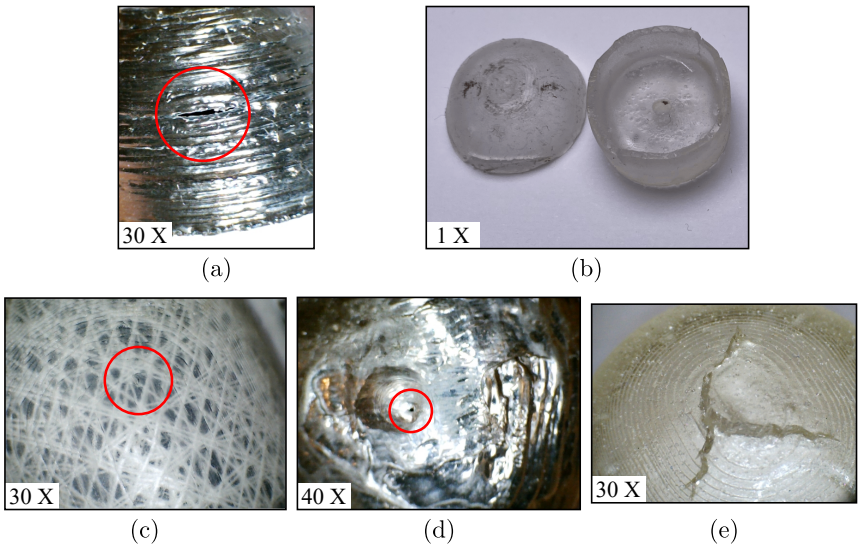

Figure 14: Types of damage incurred to SPSC during testing. Minor damages are marked with red circles. (a) Recreus TPU 60A, fatigue test. (b) Formlabs Elastic 50A, fatigue test. (c-e) Damage from puncture tests for Easy Composites AS40, Recreus TPU 60A and Formlabs Elastic 50A.

Table 3: Experimental results and performance comparison with other works

Parameter	**Tawk et al. (2019)**[1]	**Present work**			
		Type A	**Type B**	**Type C**	**Type D**
material	NinjaFlex TPU 85A (NinjaTek)	Filaflex TPU 60A PRO (Recreus)			
wall thickness	0.8 mm	1 mm			
initial gauge pressure	0 kPa	ranging from 0 to 50 kPa			
auxiliary reservoir	N/A	40 cm^3			
stiffness (low stiffness condition)[2]	N/A	min: 2.2 N/mm @ $y_s = 0$ mm max: 6.7 N/mm @ $y_s = 9$ mm mean: 4.7 N/mm	min: 1.6 N/mm @ $y_s = 1.3$ mm max: 12.5 N/mm @ $y_s = 9$ mm mean: 5.1 N/mm	min: 1.5 N/mm @ $y_s = 1.4$ mm max: 16.7 N/mm @ $y_s = 10$ mm mean: 5.0 N/mm	min: 1.8 N/mm @ $y_s = 0$ mm max: 5.9 N/mm @ $y_s = 7.2$ mm mean: 4.1 N/mm
stiffness (high stiffness condition)[2]	N/A	min: 1.5 N/mm @ $y_s = 0$ mm max: 19.8 N/mm @ $y_s = 10$ mm mean: 8.9 N/mm	min: 0.7 N/mm @ $y_s = 1.2$ mm max: 15.7 N/mm @ $y_s = 8.4$ mm mean: 7.3 N/mm	min: 1.7 N/mm @ $y_s = 1$ mm max: 22.1 N/mm @ $y_s = 10$ mm mean: 7.4 N/mm	min: 1.8 N/mm @ $y_s = 0$ mm max: 21.3 N/mm @ $y_s = 10$ mm mean: 9.2 N/mm
pressure sensitivity (low stiffness condition)[2]	N/A	min: 0.14 kPa/mm @ $y_s = 0$ mm max: 1.12 kPa/mm @ $y_s = 10$ mm mean: 0.52 kPa/mm	min: 0.11 kPa/mm @ $y_s = 0$ mm max: 0.94 kPa/mm @ $y_s = 6.7$ mm mean: 0.55 kPa/mm	min: 0.00 kPa/mm @ $y_s = 0$ mm max: 0.57 kPa/mm @ $y_s = 6.4$ mm mean: 0.33 kPa	min: 0.20 kPa/mm @ $y_s = 0$ mm max: 1.25 kPa/mm @ $y_s = 10$ mm mean: 0.72 kPa/mm
pressure sensitivity (high stiffness condition)[2]	constant	min: 1.09 kPa/mm @ $y_s = 0$ mm max: 18.67 kPa/mm @ $y_s = 10$ mm mean: 7.00 kPa/mm	min: 1.23 kPa/mm @ $y_s = 0$ mm max: 13.79 kPa/mm @ $y_s = 8.3$ mm mean: 6.44 kPa/mm	min: 0.79 kPa/mm @ $y_s = 0$ mm max: 17.25 kPa/mm @ $y_s = 10$ mm mean: 6.37 kPa/mm	min: 1.31 kPa/mm @ $y_s = 0$ mm max: 17.74 kPa/mm @ $y_s = 10$ mm mean: 7.19 kPa/mm
pressure hysteresis	negligible	negligible			
force hysteresis	N/A	8.1 N	3.8 N	4.0 N	4.5 N
lifetime	60000 cycles ($p_i = 0$ kPa)	N/A	4100 cycles ($p_i = 50$ kPa)	N/A	N/A

[1] Soft Pneumatic Push Buttons (SPPB) are considered for comparison

[2] Stiffness and pressure sensitivity values for the present work are calculated for an initial gauge pressure of 10 kPa